THE ASTROPHYSICAL JOURNAL SUPPLEMENT SERIES, 93:125–143, 1994 July

OPTICAL SPECTROPHOTOMETRY OF BLAZARS[1]

R. FALOMO
Osservatorio Astronomico di Padova, via Osservatorio 5, 35122, Padova, Italy
R. SCARPA
Dipartimento di Astronomia, Universitá di Padova, via Osservatorio 5, 35122, Padova, Italy
AND
M. BERSANELLI
Istituto di Fisica Cosmica, CNR, via Bassini 15, 20133 Milano, Italy
Received 1993 July 2; accepted 1993 September 29

ABSTRACT

We present optical spectrophotometric observations for 50 blazars obtained in 13 different campaigns over a 7 year period. The spectral flux distribution is studied in terms of a power-law ($f_\nu \propto \nu^\alpha$) and, when relevant, the contribution of a host galaxy. We give spectral indices and fluxes of the nonthermal component and, when detectable, the absolute magnitude of the host galaxy. For more than half of the objects we obtained sufficient observations to study the relation between spectral index and flux level.

Subject headings: BL Lacertae objects: general — galaxies: photometry

1. INTRODUCTION

Blazars are strong, extragalactic radio sources identified in the optical with rapidly variable and polarized sources. Their radio to ultraviolet emission is markedly nonthermal (Impey & Neugebauer 1988) and it is generally thought to be characterized by orientation effects due to plasma moving outward at relativistic velocities, as suggested by superluminal expansion (Choen et al. 1977; see also the review by Bregman 1990).

Objects exhibiting strong emission lines are usually referred to as optically violently variable (OVV) or highly polarized quasars (HPQ), while those with featureless continuum are classified as BL Lac objects. In order to understand the emission processes it is of great interest to study the spectral flux distribution over a large frequency range and to monitor the evolution of its shape and flux level.

In this paper we present a large data set of optical spectrophotometric observations of 50 blazars which were secured in a 7 year observation program. The observations were obtained using the same equipment and analyzed following a uniform procedure to ensure high homogeneity of the results. Most of the sources were observed repeatedly and in different states thus allowing a comparison of the spectral shape as observed at different flux levels.

At variance with other optical monitoring programs, which usually report broad band photometric measurements, we performed spectrophotometry in the range 4000 to 8000 Å, which enables us to better determine the spectral shape, and, particularly, to study the spectral features related to the host galaxy.

Some of these observations have been already published, as they were collected simultaneously with near-IR and/or ultraviolet data to investigate the emission distribution in a wider spectral range (Falomo et al. 1993a,b). In § 2 we present the program objects and describe the observations. Section 3 reports the results for spectral index, flux variability, and absolute magnitudes of the host galaxy; a representative spectrum of each source is also provided. In § 4 we give a description of individual objects.

2. OBSERVATIONS AND DATA ANALYSIS

The observations were obtained at the European Southern Observatory (ESO), La Silla, Chile, from 1984 November to 1991 February, on 13 different observing campaigns at typically 6 months interval (see Table 1). Two telescopes were used: the 2.2 m and the 1.5 m, both equipped with a Boller & Chivens spectrograph. Different spectrographic cameras were used for the observations at the 1.5 m obtained before and after August 1990. This resulted in a slightly better signal to noise ratio for the spectra obtained after 1990 August. As a detector we used an Image Dissector Scanner (IDS) for the observations until 1989 August and a CCD (RCA chip with 15 μm pixel^{-1}) after this time. Spectra cover the range 4000–8000 Å at a resolution of 15–20 Å (FWHM). Standard data reduction procedures were adopted to obtain one-dimensional wavelength calibrated extracted spectra. All the measurements were secured through a 8×8 arcsec^2 effective aperture. Spectra were calibrated in absolute flux units using several observations of spectrophotometric standard stars (Stone 1977) obtained on the same night. Fluxes have been corrected for Galactic extinction according to the interstellar extinction law of Cardelli, Clayton, & Mathis (1989). The value of A_V for each objects were derived assuming $R = 3.09 \pm 0.06$ (Rieke & Lebofsky 1985), and for the gas to dust ratio we have adopted the result of the *IUE* Lyα survey (Shull & Van Steenberg 1985): $N_H/E(B-V) = 5.2 \times 10^{21}$. The hydrogen column density was determined either interpolating the grid of the Bell Lab Survey (Stark et al. 1992) or, when available, using the accurate narrow beam (21′) measurement of N_H in the direction of

[1] Based on observations collected at the European Southern Observatory, La Silla, Chile.

TABLE 1

CAMPAIGNS OF OBSERVATION

Dates	Telescope	Detector
1984 Nov 8,9,10,11,12	ESO 1.5	IDS
1986 Aug 16,17,18,19	ESO 2.2	CCD
1986 Sep 8,9,10,11	ESO 1.5	IDS
1987 Jan 7,8,9,10	ESO 1.5	IDS
1987 Aug 25,26,27,28,29,30	ESO 1.5	IDS
1988 Jan 7,8,9,10,11	ESO 1.5	IDS
1988 Aug 4,6,7,8,9,10,11,12,13	ESO 1.5	CCD
1988 Dec 30,31	ESO 2.2	CCD
1989 Feb 10,11,12,13	ESO 1.5	CCD
1989 Aug 6,7,8,9,10,11	ESO 1.5	CCD
1990 Feb 17,18,19	ESO 2.2	CCD
1990 Sep 17,18,19,20	ESO 1.5	CCD
1991 Feb 11,12,13,14	ESO 1.5	CCD

several active galactic nuclei (AGNs) from Elvis, Lockman, & Wilkes (1989).

Objects observed are somewhat heterogeneous and do not satisfy any completeness criterion, the only selection parameters being observability from La Silla and detectability. In total we have obtained data for 50 blazars. The sample is composed of 37 classical BL Lac objects while another 13 show emission lines with rest frame equivalent width greater than 5 Å and following the Moore & Stockmann (1981) criterion are classified as OVV or HPQ.

Program objects are reported in Table 2. The columns give: (1) coordinate name; (2) other names or catalog; (3) and (4) right ascension and declination; (5) redshift; (6) interstellar extinction A_V; (7) presence of a relevant emission from the host galaxy; (8) classification of the object as X-ray selected (radio-weak objects) or radio selected (radio-strong objects) following the criteria of Ledden & O'Dell (1985); (9) presence of strong (E.W. > 5 Å) emission lines.

3. RESULTS

We report in Figure 1 a representative spectrum for each program object. As apparent from simple inspection of Figure 1 the spectral flux distribution in most cases appears well described by a single power law ($f_\nu \propto \nu^\alpha$). Additional components such as those from the starlight of the host galaxy and possibly other thermal contributions are visible only in a limited number of sources. Emission lines are also present for OVV and HPQ blazars.

For all observations we have derived a spectral index α which results either from the best fit to the data with a single power law or from the decomposition into a power law plus the host galaxy emission. The host galaxy was assumed to be a standard elliptical (Yee & Oke 1978), and its significance is quantified by the fraction P_g of the flux due to the host galaxy with respect to the total observed flux at 5500 Å. An automated procedure was implemented in order to obtain the best decomposition, varying the relative contribution of the host galaxy with respect to the power law component. Emission lines in the spectrum and telluric absorption were removed by the procedure. The uncertainty in the determination of α and P_g depends on the relative contribution of the two components, α being better determined for smaller P_g. Typically we found uncertainties of 0.1–0.3 for α and 0.1–0.25 for P_g. From the measured thermal flux and the redshift we can also estimate the absolute magnitude M_V of the host galaxy. Generally we found consistent values of M_V from decomposition of different spectra of the same object. In Table 3 we report for each observation the Modified Julian Date (MJD), the observed flux at 5500 Å, the spectral index α and, when relevant, P_g. For all objects where stellar emission was detected we also give, in Figure 2, a representative decomposition of the spectrum showing the power law and host galaxy components as well as the best fit to the data.

In Table 4 we summarize the results. Columns (2) and (3) report the number of observations (N_O) for each object and the number of observing campaigns (N_C). Significant flux variability is observed for the most monitored objects. The average flux for each object at 5500 Å, $\langle F_\nu \rangle$, and the variability parameter $\phi \equiv (F_{\max} - F_{\min})/F_{\min}$, are reported in columns (4) and (5). We found $\phi \gtrsim 2$ for 11 objects and $\phi \gtrsim 1$ for 23 objects. In spite of large flux variability the spectral index α usually exhibits small variations. In Table 4 (cols. [6], [7], and [8]) we report the weighted average spectral index $\langle \alpha \rangle$ together with its maximum and minimum values. A histogram of the distribution of $\langle \alpha \rangle$ is also shown in Figure 3. The mean of the distribution is -0.98 ± 0.43 (the quoted error indicates the 1 σ dispersion of the distribution).

In our sample of blazar it is possible to consider four groups (see Table 2): classical BL Lac objects (weak emission lines objects) (37 sources), objects with strong emission lines (13 sources), radio selected objects (40 sources) and X-ray selected objects (10 sources). We found that radio selected and X-ray selected blazar have significantly different mean spectral index, respectively $\langle \alpha \rangle = -1.05 \pm 0.42$ and $\langle \alpha \rangle = -0.65 \pm 0.30$. The two distributions are distinct at the 99% significance level by a Kolmogorov-Smirnov test both using all objects and all but PKS 2208−137 (the only source with $\alpha > 0$). The strong emission line objects and weak emission line objects also have different mean spectral index, respectively $\langle \alpha \rangle = -0.75 \pm 0.57$ and $\langle \alpha \rangle = -1.05 \pm 0.35$ (see Fig. 3). However the two distributions are only marginally distinct, at 87% significance level, and if we exclude PKS 2208−137 the two distributions are indistinguishable. In Table 5 we summarize the average spectral indices for these groups.

For each object observed in more than two campaigns and with at least five photometric observations, we have studied the correlation between the flux level and spectral index. In column (9) of Table 4 we give the Spearman rank-order coefficient. Possible correlation is shown for the objects 0048−097, 0138−097 and 0338−215. However, in no cases are the results compelling or conclusive. On the other hand, for a number of sources a remarkable stability of the spectral index is observed even under large ($\phi \gtrsim 2$) flux level variations.

Finally, for those objects which exhibited a host galaxy we report in Table 4 (cols. [8] and [9]) the range of values of P_g and the average value of M_V of the host galaxy as derived from the decomposition of the spectrum (all values are computed assuming $q_0 = 0$ and $H_0 = 50$ km s^{-1} Mpc^{-1}).

Some details on individual objects are given in the next section.

TABLE 2

PROGRAM OBJECTS

Object (1)	Name (2)	α (1950) (3)	δ (1950) (4)	z (5)	A_V (6)	Gal (7)	X/R (8)	E.L. (9)
0048 − 097	PKS	004810	−094524	···	0.21	N	R	N
0109 + 225	S2	010924	222844	···	0.27	N	R	N
0118 − 273	PKS	011809	−271707	> 0.569	0.09	N	R	N
0138 − 097	OC −065	013857	−094351	> 0.501	0.17	N	R	N
0215 + 015	OD +026	021514	013100	1.72	0.21	N	R	Y
0301 − 243	OE −202	030116	−242200	···	0.11	N	R	N
0323 + 022	H,1H,1ES	032338	021447	0.147	0.50	Y	X	N
0338 − 214	OE −263.9	033823	−212908	···	0.16	N	R	N
0414 + 009	1H, 87GB	041418	005803	0.287	0.51	Y	X	N
0422 + 005	PKS	042213	002917	···	0.42	N	R	N
0521 − 365	ESO 362-G021	052113	−363016	0.055	0.21	Y	R	Y
0537 − 441	PKS	053721	−440640	0.894	0.20	N	R	N
0548 − 323	4U,H,1H,ES	054850	−321656	0.069	0.14	Y	X	N
0735 + 178	PKS	073514	174909	> 0.424	0.28	N	R	N
0736 + 017	PKS	073643	014400	0.191	0.72	N	R	Y
0754 + 101	MRC,OI+090.4	075422	100440	···	0.16	N	R	N
0808 + 019	HB89,OJ+014	080851	015550	···	0.25	N	R	N
0818 − 128	OJ−131	081836	−124925	···	0.45	N	R	N
0823 + 033	OJ+038,PKSB	082314	031916	0.506	0.22	N	R	N
0823 − 223	PKS	082350	−222035	> 0.910	0.62	N	R	N
0829 + 046	OJ+049	082911	043951	0.18	0.18	Y	R	N
0836 + 182	HB89, 87GB	083640	181325	···	0.19	N	R	N
0851 + 203	OJ 287	085157	201758	0.306	0.18	N	R	Y
0906 + 016	PKS,4C,DA263	090635	013348	1.018	0.22	N	R	Y
1020 − 104	OL−133,PKS	102004	−102234	0.197	0.30	N	R	Y
1055 + 018	DA293,PKS,4C	105555	015004	0.888	0.23	N	R	Y
1057 + 101	MRC,HB89	105743	100542	1.317	0.15	N	R	Y
1101 − 232	2A,3A,4U,1H	110111	−231320	0.186	0.34	Y	X	N
1144 − 379	MRC, PKS	114431	−375531	1.048	0.52	N	R	N
1244 − 255	HB89, PKS	124407	−253126	0.638	0.42	N	R	Y
1309 − 217	HB89, MC1	130950	−214029	> 1.489	0.49	N	R	N
1400 + 162	VRO 16.14.01	140020	161421	0.245	0.10	Y	R	N
1402 + 042	1E,MS	140220	041621	···	0.13	N	X	N
1407 + 022	OQ+012,PKS	140732	021715	···	0.16	N	R	N
1514 − 242	AP Lib	151445	−241122	0.049	0.52	Y	R	N
1519 − 273	PKS	151937	−271930	···	0.55	N	R	N
1538 + 149	4C 14.60	153831	145725	0.605	0.19	N	R	N
1553 + 113	PG	155321	112004	···	0.21	N	X	N
1722 + 119	H,4U,87GB	172244	115452	···	0.51	N	X	N
1749 + 096	OT+081	174910	093943	0.322	0.57	N	R	Y
2005 − 489	PKS,1ES	200546	−485843	0.071	0.33	Y	X	N
2012 − 017	PKSB,PKS	201239	−014646	···	0.52	N	R	N
2155 − 304	PKS,1H,2A,3A	215558	−302752	0.116	0.11	N	X	N
2201 + 044	PKS	220144	042605	0.028	0.29	Y	R	N
2208 − 137	PKS	220843	−134259	0.392	0.20	N	R	Y
2223 − 052	3C 446	222311	−051217	1.404	0.33	N	R	Y
2230 + 115	PKS	223008	112824	···	0.36	N	R	Y
2240 − 260	OY−268, PKS	224042	−260015	0.774	0.09	N	R	N
2254 + 074	OY+091,MG	225446	072709	0.190	0.32	Y	R	N
2356 − 309	U, 4U	235634	−305421	0.165	0.08	Y	X	N

4. NOTES ON INDIVIDUAL OBJECTS

0048−097.—We obtained, over seven campaigns, 14 spectra of this bright ($m_V \simeq 15$) radio-selected source confirmed as a blazar by Angel & Stockman (1980). No indication of spectral features either in emission or absorption was found. The flux has shown variations as large as 200%. All the spectra are well described by a power-law model from 4000 to 8000 Å even at minimum flux level. The spectral index shows variations of up to 0.8 correlating with flux variations in the sense that when the flux increases the spectral index is flatter. The significance level is 95% for a Spearman's test. However, the errors on α are quite large and, if we consider that Ballard et al. (1990) found opposite results (spectral index increases with flux), it is obvious that more accurate observations are necessary to clarify the issue.

0109+225.—We obtained three spectra of this radio selected source. All spectra are compatible with a power-law

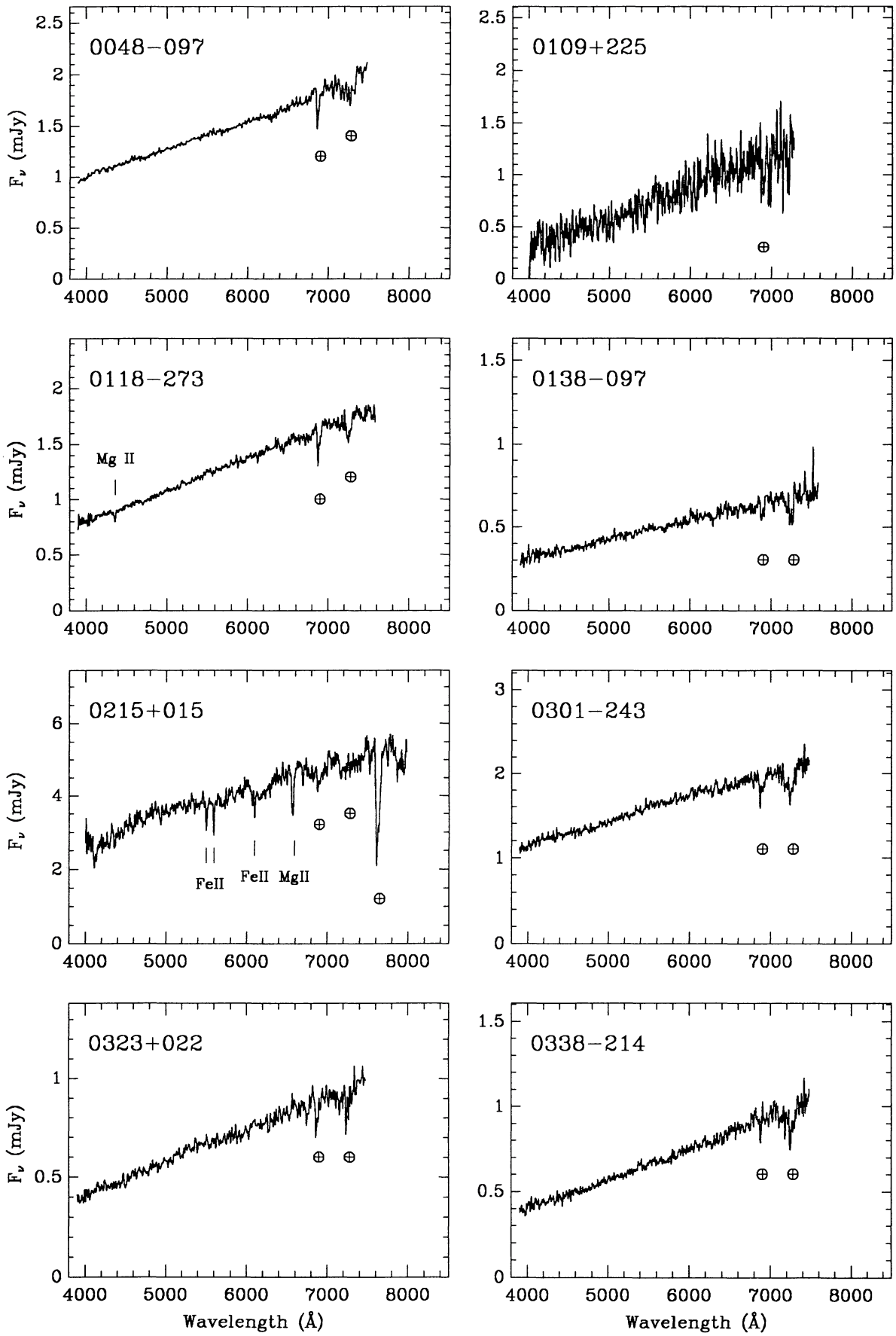

FIG. 1.—Representative spectrum of each program object, sorted by right ascension. Spectra plotted are those marked with an asterisk (*) in Table 3. Atmospheric absorption bands (⊕) and main features are marked.

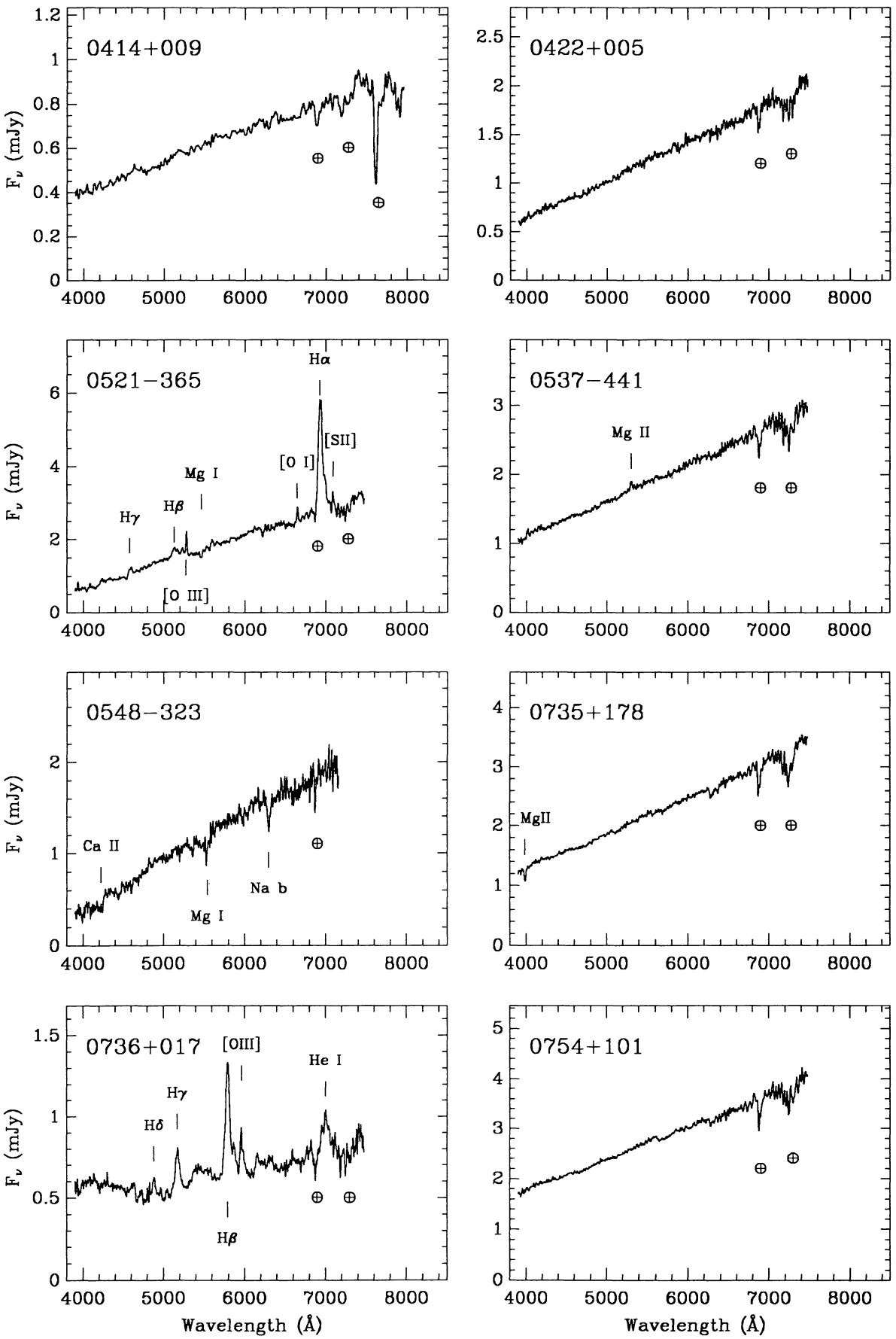

FIG. 1—*Continued*

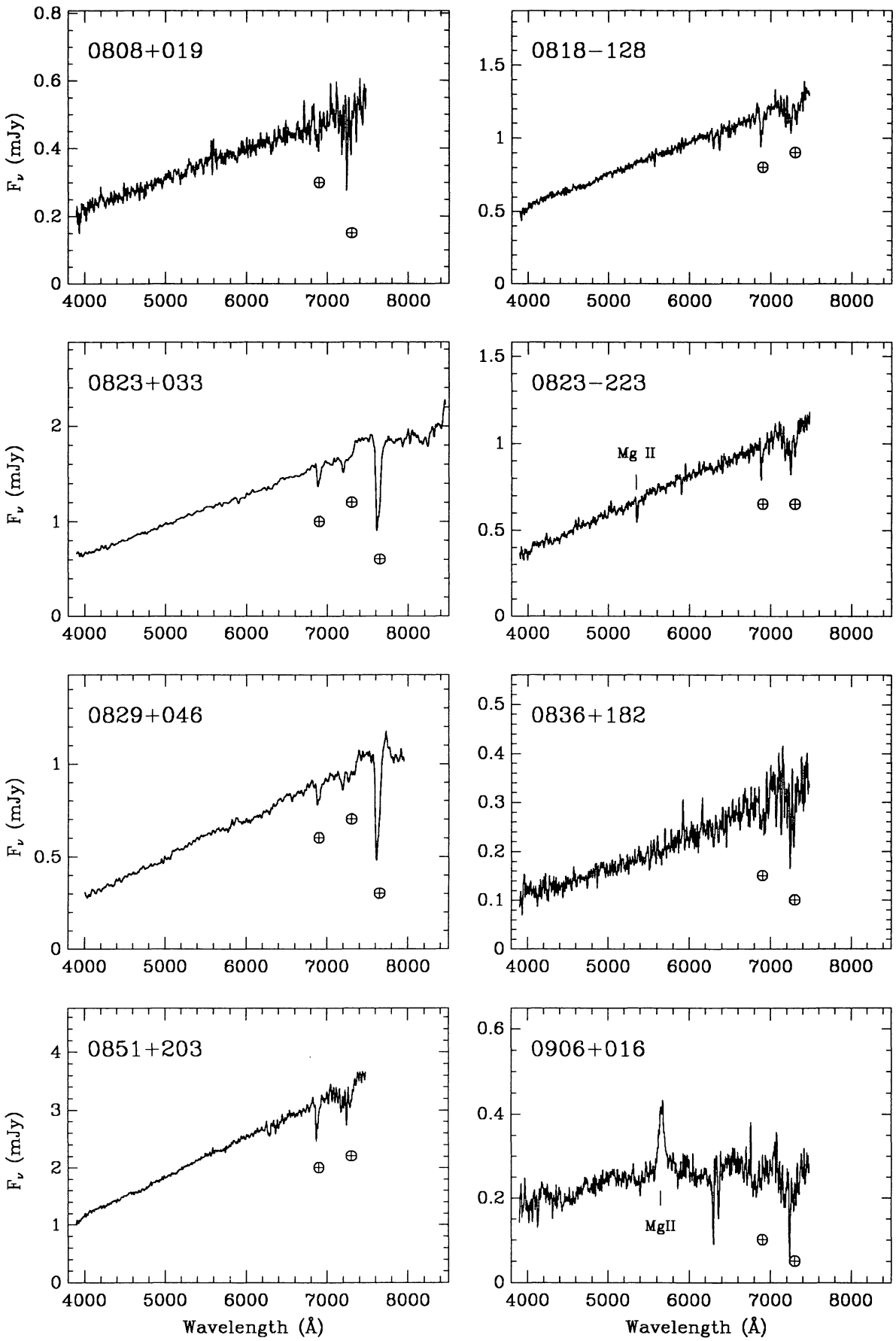

FIG. 1—*Continued*

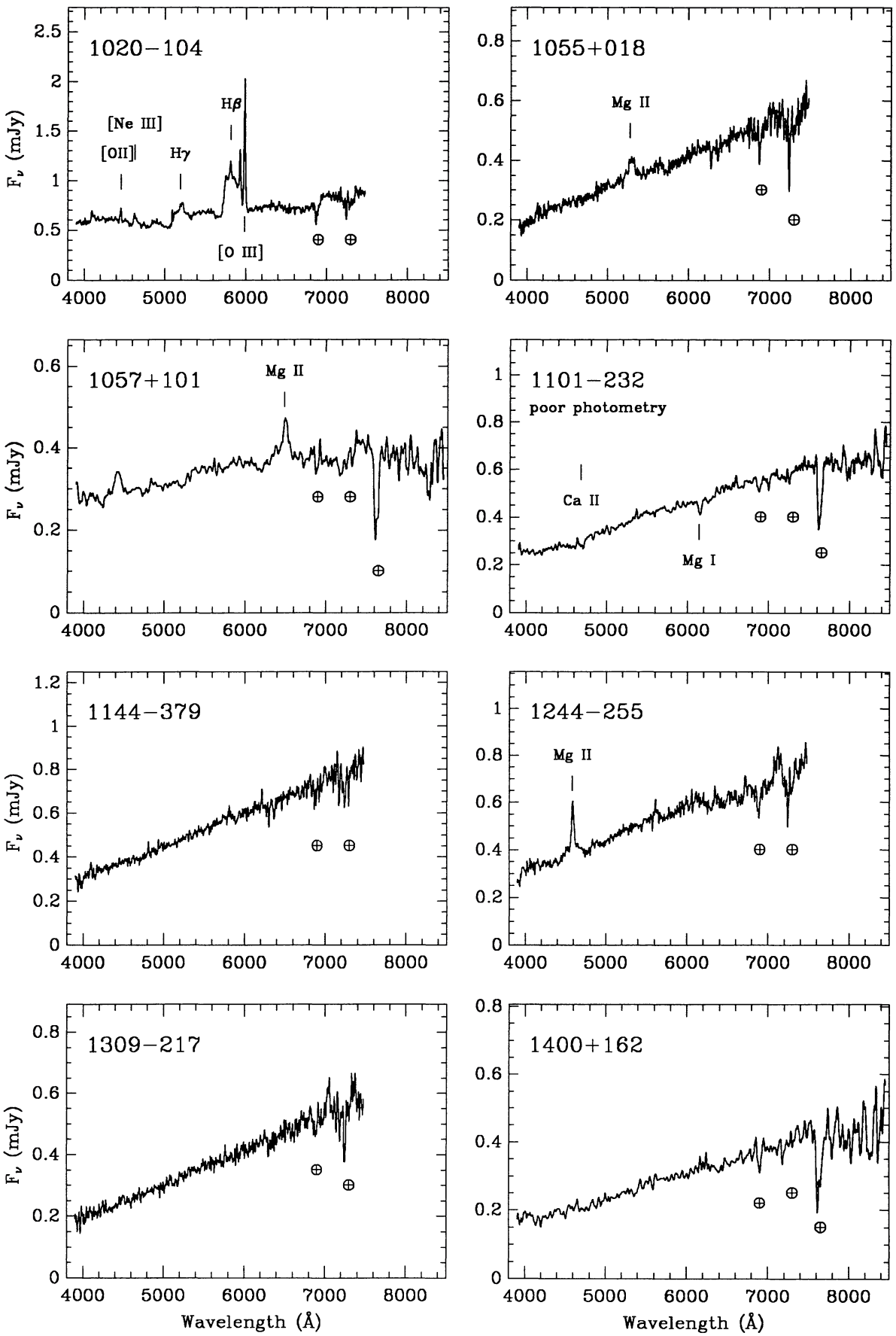

FIG. 1—*Continued*

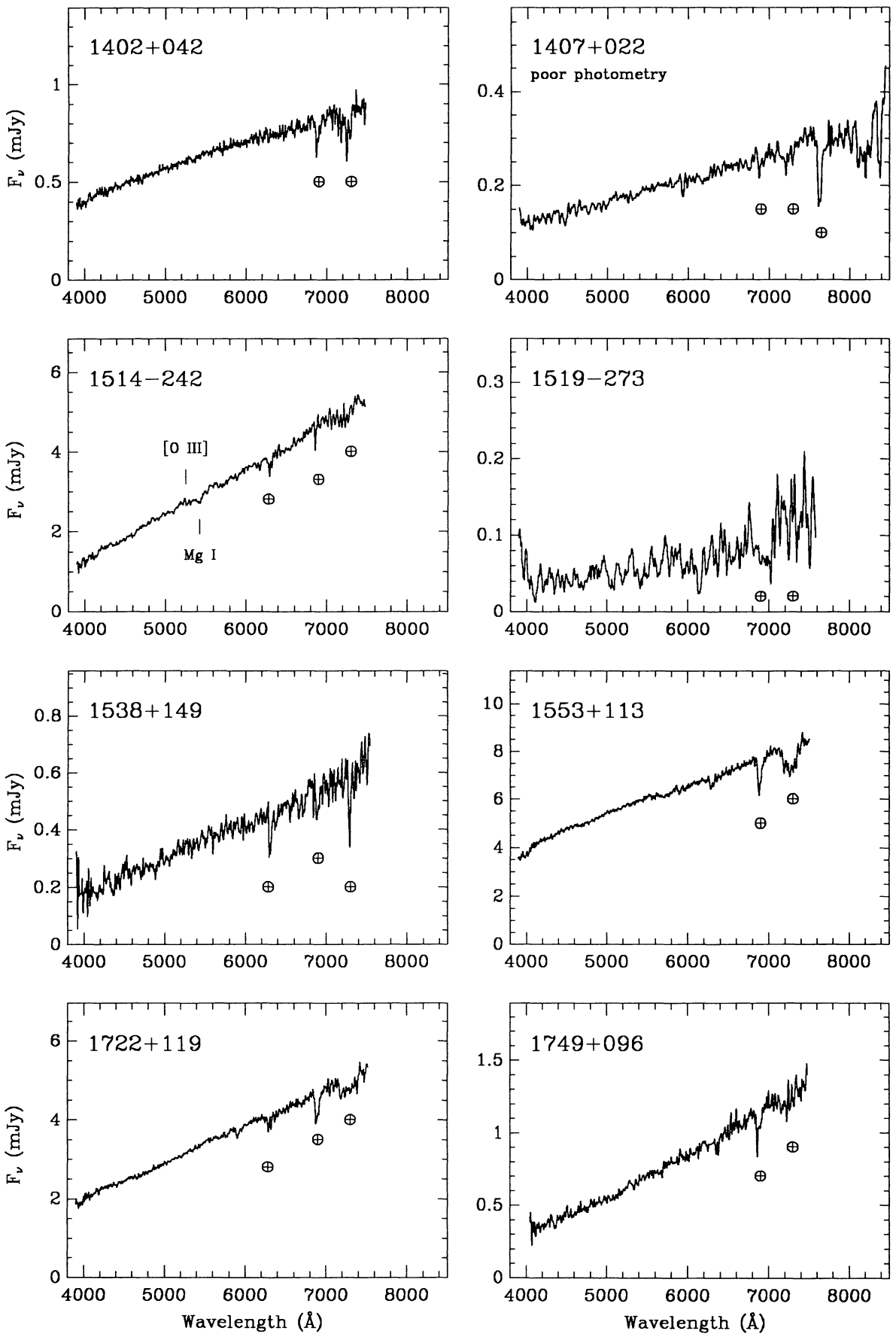

FIG. 1—*Continued*

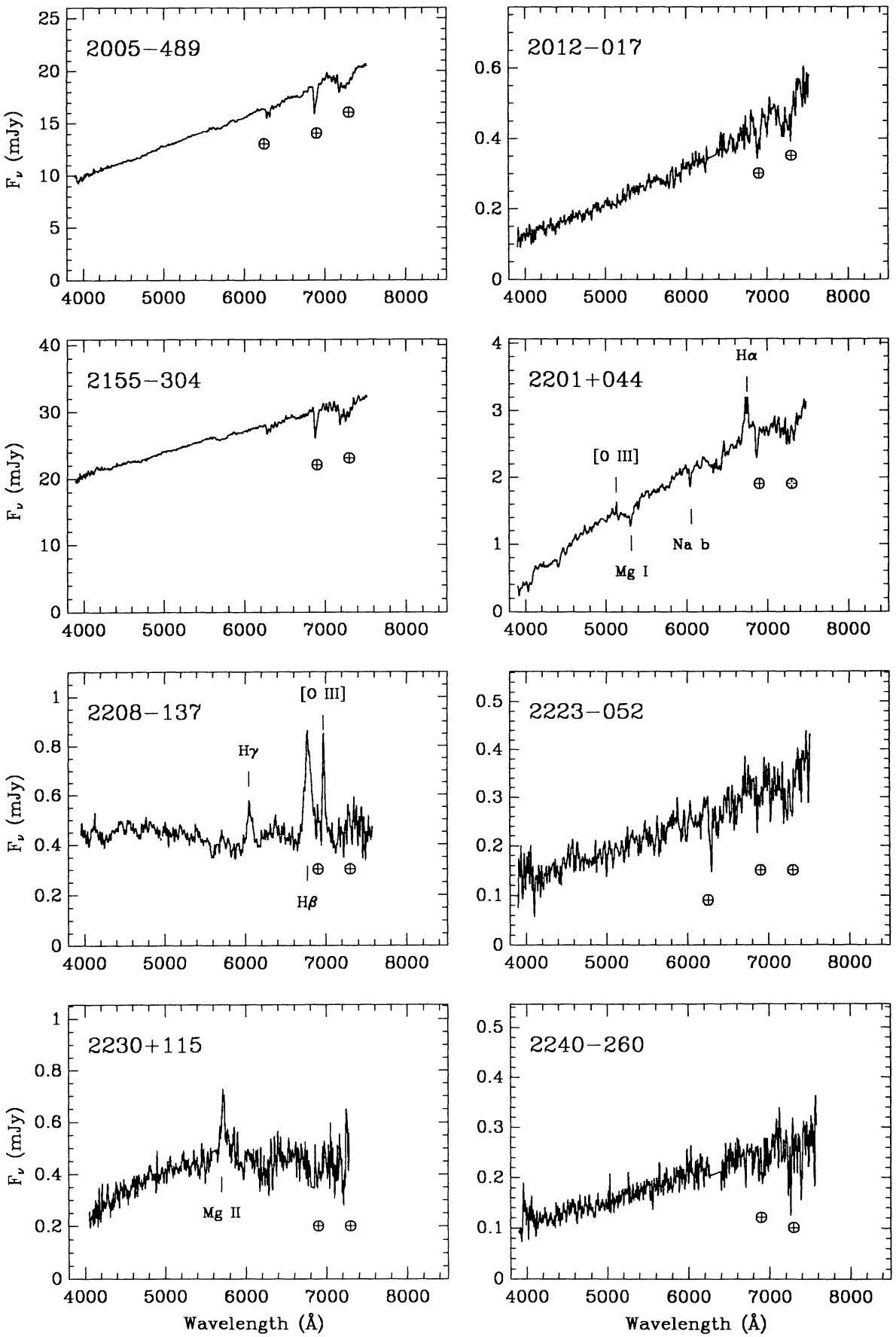

FIG. 1—*Continued*

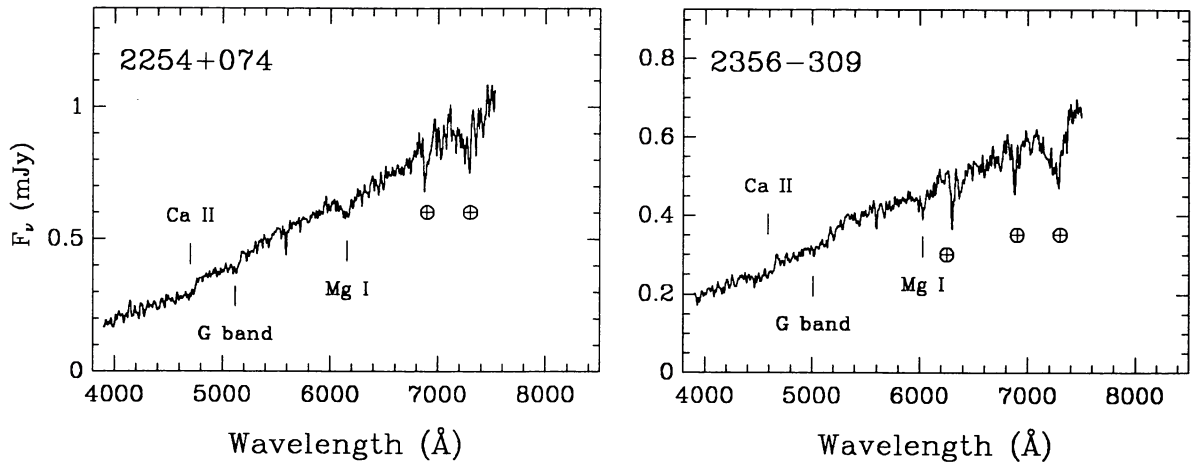

FIG. 1—*Continued*

model. Flux emission shows variations with amplitude up to $\simeq$1.3 magnitudes.

0118−273.—Ten spectra were secured for this radio-selected BL Lac object. The optical emission is smooth and well represented by a power law. Only a weak absorption line is present, which was identified as Mg II (2798 Å) at $z = 0.557$ (Falomo 1991b). Flux variability was detected on short time scales, with a variation of 100% in 3 days. The spectral index has shown some variation with a maximum $\Delta\alpha = 0.55$.

0138−097.—The optical spectrum of this radio selected object shows only an absorption line visible at low emission level (probably Mg II 2798 Å as noted by Stickel et al. 1993). The spectral index remains nearly constant ($\Delta\alpha = 0.28$) despite flux variation of more than 100%. Even though the variations of α are compatible with a constant spectral index, they seem to be correlated to the flux level at a 90% significance level; more accurate observations, and an extension of the observed flux level range, are necessary.

0215+015.—This radio-selected source is one of the most distant ($z = 1.72$ Boissé & Bergeron 1988) BL Lac objects known. Some intervening narrow absorption lines are present in our spectra but no emission lines are detected, probably because we observed the source in a brighter state compared to the one observed by Boissé & Bergeron (1988), who found weak C IV emission lines. The energy distribution is compatible with a single power-law model.

0301−23.—We have obtained six spectra of this radio selected object, discovered on the basis of its polarimetric properties (Impey & Tapia 1988). We observed flux variations of more than 100% while the spectral index remained practically unchanged.

0323+022.—This X-ray selected object, discovered in the *HEAO 1* all-sky survey, was classified as a blazar by Feigelson et al. (1986) who noted its rapid variability. The optical energy distribution exhibits the signature of stellar emission with a typical contribution of 25%, corresponding to an absolute magnitude of the host galaxy of $M_V = -22.1 \pm 0.4$. This value is in good agreement with the values of $M_V = -22$ found by Falomo et al. (1993a) based on simultaneous optical to near-IR observations, and of $M_V = -22.5 \pm 0.7$ found by Feigelson et al. (1986).

0338−215.—This source was identified with a featureless optical radio source by Wilkes et al. (1983). We obtained six spectra; none show features. The optical spectrum is well fitted by a power law with constant ($\Delta\alpha \lesssim 0.2$) spectral index.

0414+009.—We obtained six spectra of this X-ray selected source, classified as a BL Lac object by Ulmer et al. (1983). We found that the contribution of the stellar emission due to the host galaxy is, on average, $P_g = 0.08$, corresponding to an absolute magnitude $M_V = -22.2 \pm 0.5$.

0422+005.—This is a typical radio-selected BL Lac object showing featureless spectra (Wills & Wills 1976), large flux and polarization variability (Mead et al. 1990). We have repeatedly observed this source, obtaining 12 spectra at very different flux levels. No features were found in the spectra, all of which follow a power law very well. The flux varied by a factor of 3 while the spectral index remained relatively stable ($\Delta\alpha \lesssim 0.5$).

0521−365.—This blazar is a powerful radio source and is remarkable for its optical jet (Danziger et al. 1979; Boisson, Cayatte, & Sol 1989). The spectra show strong broad and narrow emission lines at $z = 0.055$. The Balmer lines are broad with FWHM $\simeq$ 3000 km s^{-1} for H_α, who have variable equivalent width. The forbidden lines of [O III], partially blended with H_β, are strong and narrow with FWHM $\simeq$ 600 km s^{-1}. Flux variations up to a factor of 2 are seen on short and long timescales. The energy distribution clearly exhibits the presence of a strong thermal component which contributes 55% of the total emission. The absolute magnitude of the host galaxy is $M_V = -21.6 \pm 0.2$, fully consistent with $M_V = -21.7$ found in the optical to near-IR range (Falomo et al. 1993a). The spectral index varied from -0.87 to -1.62 with no apparent correlation with flux variations.

0537−441.—This blazar is strongly variable in the optical domain (Impey & Tapia 1988). We obtained 14 spectra of the source over 7 years finding a maximum flux variation of 1.6 magnitudes, and a variation of 0.25 magnitudes in 1 day. All spectra are well described by a power-law model. The spectral index showed variations of up to $\Delta\alpha \simeq 0.6$.

0548−323.—We obtained four photometric spectra, at nearly the same flux level, of this bright X-ray selected object (Impey & Neugebauer 1988). The host galaxy emission con-

TABLE 3

JOURNAL OF OBSERVATIONS

Name	MJD	F_ν (mJy)[3)]	α	P_g	
0048 − 097	46684.277	0.81 ± 0.03	−1.14 ± 0.13	...	
	46803.090	2.43 ± 0.13	−0.82 ± 0.15	...	
	46804.074	2.34 ± 0.15	−0.72 ± 0.23	...	
	47033.266	1.21 ± 0.11	−1.35 ± 0.28	...	
	47033.289	...	−1.30 ± 0.56	...	
	47035.211	1.41 ± 0.17	−1.51 ± 0.38	...	
	47036.207	1.48 ± 0.16	−1.33 ± 0.29	...	
	47167.066	1.07 ± 0.08	−1.09 ± 0.19	...	
	47170.039	0.89 ± 0.07	−1.05 ± 0.25	...	
	47376.359	1.51 ± 0.08	−1.04 ± 0.18	...	
	47377.336	1.49 ± 0.05	−0.81 ± 0.15	...	
	47526.074	2.28 ± 0.08	−0.92 ± 0.18	...	
	47746.320	1.54 ± 0.02	−0.94 ± 0.05	...	
	47749.281	1.42 ± 0.04	−0.86 ± 0.05	...	*
0109 + 225	46016.086	0.47 ± 0.10	−0.74 ± 0.55	...	
	46682.250	1.51 ± 0.07	−1.06 ± 0.13	...	
	47034.305	0.83 ± 0.14	−0.72 ± 0.50	...	*
0118 − 273	47034.359	1.30 ± 0.11	−1.39 ± 0.30	...	
	47037.207	1.76 ± 0.14	−1.14 ± 0.22	...	
	47167.094	1.32 ± 0.10	−0.84 ± 0.27	...	
	47168.043	1.79 ± 0.08	−0.98 ± 0.12	...	
	47377.371	1.57 ± 0.06	−1.36 ± 0.13	...	
	47745.336	1.17 ± 0.02	−1.21 ± 0.05	...	
	47748.289	1.36 ± 0.02	−1.23 ± 0.05	...	
	47750.348	...	−1.12 ± 0.05	...	
	48152.301	1.23 ± 0.02	−1.22 ± 0.05	...	*
	48155.191	0.68 ± 0.06	−1.18 ± 0.25	...	
0138 − 097	47035.277	0.98 ± 0.11	−0.96 ± 0.33	...	
	47168.086	1.11 ± 0.06	−0.85 ± 0.15	...	
	47377.258	0.55 ± 0.01	−1.02 ± 0.05	...	
	47746.359	0.64 ± 0.02	−1.04 ± 0.08	...	
	47749.328	0.55 ± 0.01	−1.01 ± 0.05	...	
	48152.348	0.48 ± 0.02	−1.13 ± 0.13	...	*
0215 + 015	46015.133	3.68 ± 0.31	−0.63 ± 0.11	...	*
	46017.148	4.17 ± 0.19	−0.77 ± 0.08	...	
0301 − 244	47526.109	1.33 ± 0.05	−1.04 ± 0.20	...	
	47745.363	1.19 ± 0.01	−1.12 ± 0.05	...	
	47748.324	1.09 ± 0.02	−1.23 ± 0.05	...	
	47942.148	...	−0.88 ± 0.05	...	
	48155.277	0.76 ± 0.02	−0.91 ± 0.10	...	
	48299.043	1.61 ± 0.03	−0.90 ± 0.07	...	*
0323 + 022	47169.047	0.81 ± 0.06	−0.22 ± 0.25	0.33	
	47745.398	0.67 ± 0.01	−0.25 ± 0.20	0.19	*
	47749.367	0.79 ± 0.02	−0.26 ± 0.20	0.23	

Name	MJD	F_ν(mJy)	α	P_g	
0338 − 215	47171.129	0.96 ± 0.07	−1.51 ± 0.24	...	
	47379.352	0.88 ± 0.05	−1.51 ± 0.24	...	
	47748.359	0.80 ± 0.01	−1.51 ± 0.05	...	
	47942.184	...	−1.30 ± 0.05	...	
	48301.027	0.68 ± 0.03	−1.31 ± 0.10	...	
	48302.043	0.66 ± 0.02	−1.32 ± 0.09	...	*
0414 + 009	47379.406	0.58 ± 0.08	−0.19 ± 0.35	0.15	
	47569.031	0.65 ± 0.06	−0.50 ± 0.30	0.05	
	47747.375	0.69 ± 0.01	−0.61 ± 0.20	0.05	
	47749.402	0.72 ± 0.01	−0.15 ± 0.20	0.10	
	47939.039	0.62 ± 0.01	−0.47 ± 0.20	0.05	*
	48301.070	0.57 ± 0.02	−0.27 ± 0.20	0.05	
0422 + 005	46683.305	2.52 ± 0.10	−1.40 ± 0.08	...	
	46804.117	1.55 ± 0.12	−1.29 ± 0.20	...	
	47035.406	0.65 ± 0.09	−1.45 ± 0.37	...	
	47169.133	2.27 ± 0.07	−1.26 ± 0.08	...	
	47170.098	2.36 ± 0.06	−1.27 ± 0.07	...	
	47171.078	2.38 ± 0.08	−1.25 ± 0.09	...	
	47377.414	0.93 ± 0.05	−1.10 ± 0.20	...	
	47568.039	1.48 ± 0.08	−1.59 ± 0.17	...	
	47571.031	1.66 ± 0.08	−1.23 ± 0.13	...	
	47746.398	1.25 ± 0.03	−1.30 ± 0.05	...	
	47941.152	...	−1.46 ± 0.05	...	
	48300.035	1.28 ± 0.02	−1.36 ± 0.06	...	*
0521 − 365	46013.234	2.73 ± 0.17	−1.14 ± 0.15	0.55	
	46015.285	2.99 ± 0.17	−0.91 ± 0.15	0.50	
	46017.219	2.10 ± 0.12	−1.15 ± 0.15	0.55	
	46682.336	3.72 ± 0.13	−1.44 ± 0.15	0.47	
	46684.379	3.69 ± 0.16	−1.03 ± 0.15	0.57	
	46803.199	2.36 ± 0.16	−0.87 ± 0.15	0.65	
	46806.125	3.30 ± 0.15	−0.94 ± 0.15	0.45	
	47033.410	1.72 ± 0.21	−1.62 ± 0.35	0.55	
	47037.340	1.86 ± 0.16	−1.54 ± 0.15	0.68	
	47167.180	2.85 ± 0.18	−1.32 ± 0.15	0.57	
	47167.203	2.87 ± 0.18	−1.43 ± 0.15	0.57	
	47526.203	2.39 ± 0.15	−1.39 ± 0.15	0.57	
	47568.078	3.08 ± 0.33	−1.35 ± 0.15	0.47	
	47941.188	1.83 ± 0.02	−1.40 ± 0.15	0.60	
	48153.348	...	−1.41 ± 0.15	0.50	
	48300.066	1.78 ± 0.13	−1.09 ± 0.15	0.57	*
0537 − 441	46013.316	1.63 ± 0.13	−1.32 ± 0.31	...	
	46014.309	1.52 ± 0.10	−1.26 ± 0.19	...	
	46016.266	1.73 ± 0.12	−1.16 ± 0.20	...	
	46017.285	1.70 ± 0.08	−1.39 ± 0.13	...	
	46682.387	1.50 ± 0.07	−1.65 ± 0.13	...	
	46803.207	1.39 ± 0.04	−1.37 ± 0.09	...	
	46805.184	1.42 ± 0.07	−1.35 ± 0.14	...	

TABLE 3—*Continued*

Name	MJD	F_ν(mJy)	α	P_g		Name	MJD	F_ν(mJy)	α	P_g	
0829 + 047	47568.207	1.46 ± 0.06	−0.83 ± 0.20	0.15		0537 − 441	47036.398	0.85 ± 0.09	−1.31 ± 0.32	...	
	47570.219	2.30 ± 0.07	−1.10 ± 0.25	0.21			47168.195	0.62 ± 0.05	−1.23 ± 0.30	...	
	47939.199	0.81 ± 0.01	−0.92 ± 0.30	0.25			47169.184	0.48 ± 0.06	−1.53 ± 0.35	...	
	47941.316	0.62 ± 0.01	−1.04 ± 0.30	0.30	*		47526.238	1.41 ± 0.04	−1.31 ± 0.10	...	
	48301.207	3.09 ± 0.02	−1.10 ± 0.15	0.13			47568.129	0.80 ± 0.06	−1.46 ± 0.19	...	
							47939.063	1.58 ± 0.01	−1.06 ± 0.05	...	
0836 + 182	48301.156	0.19 ± 0.01	−1.58 ± 0.22	...	*		48299.066	1.97 ± 0.04	−1.35 ± 0.05	...	*
0851 + 203	46804.309	1.15 ± 0.05	−1.22 ± 0.12	...		0548 − 323	46683.383	1.27 ± 0.06	−0.58 ± 0.20	0.70	
	46806.289	1.10 ± 0.05	−1.20 ± 0.12	...			46804.207	1.41 ± 0.07	−0.42 ± 0.25	0.60	
	47570.184	3.76 ± 0.06	−1.18 ± 0.05	...			47169.223	1.34 ± 0.09	−1.05 ± 0.25	0.70	
	48300.191	2.24 ± 0.02	−1.61 ± 0.05	...	*		47569.078	1.17 ± 0.07	−0.66 ± 0.25	0.66	*
							47942.219	...	−0.40 ± 0.30	0.60	
0906 + 016	48302.223	0.28 ± 0.02	−0.55 ± 0.22	...	*		48299.098	...	−0.13 ± 0.20	0.62	
1020 − 104	47568.250	0.76 ± 0.07	−0.42 ± 0.19	...		0735 + 178	46804.250	1.17 ± 0.06	−1.40 ± 0.20	...	
	47942.336	...	−0.30 ± 0.05	...			47570.074	1.06 ± 0.07	−1.28 ± 0.15	...	
	48300.234	0.72 ± 0.06	−0.14 ± 0.10	...	*		48299.133	2.21 ± 0.03	−1.23 ± 0.05	...	*
1055 + 018	47569.215	0.39 ± 0.06	−1.32 ± 0.35	...		0736 + 017	48302.160	0.73 ± 0.03	−0.08 ± 0.09	...	*
	48300.281	0.36 ± 0.01	−1.39 ± 0.13	...	*						
						0754 + 101	46015.344	1.54 ± 0.22	−1.13 ± 0.45	...	
1057 + 101	47939.242	0.35 ± 0.01	−0.58 ± 0.09	...	*		46803.270	2.52 ± 0.06	−1.24 ± 0.07	...	
	47941.383	...	−0.57 ± 0.11	...			47167.234	2.14 ± 0.12	−1.14 ± 0.13	...	
							47939.121	3.54 ± 0.02	−1.11 ± 0.05	...	
1101 − 232	47568.293	0.43 ± 0.07	−0.60 ± 0.50	0.35			48300.098	2.75 ± 0.03	−1.10 ± 0.05	...	*
	47570.289	0.57 ± 0.04	−0.66 ± 0.20	0.30							
	47571.320	0.59 ± 0.06	−0.69 ± 0.25	0.30		0808 + 019	47168.246	1.03 ± 0.07	−0.77 ± 0.22	...	
	47941.352	...	−0.44 ± 0.20	0.25	*		47170.199	0.92 ± 0.06	−0.63 ± 0.21	...	
	47942.371	...	−0.61 ± 0.20	0.20			47941.215	...	−0.94 ± 0.05	...	
	48299.289	0.56 ± 0.01	−0.25 ± 0.15	0.30			47942.254	...	−0.95 ± 0.06	...	
							48300.137	0.36 ± 0.01	−1.08 ± 0.12	...	*
1144 − 379	47171.324	0.50 ± 0.06	−1.13 ± 0.43	...							
	47569.254	0.77 ± 0.06	−1.17 ± 0.18	...		0818 − 128	46805.250	0.67 ± 0.05	−0.86 ± 0.25	...	
	48301.250	0.52 ± 0.01	−1.00 ± 0.10	...	*		47169.270	0.53 ± 0.04	−0.75 ± 0.55	...	
							47570.246	0.29 ± 0.04	−1.21 ± 0.40	...	
1244 − 255	47568.355	0.83 ± 0.06	−1.09 ± 0.20	...			47941.266	...	−0.88 ± 0.05	...	
	47942.430	...	−0.64 ± 0.36	...			48299.238	0.88 ± 0.02	−0.86 ± 0.06	...	*
	48300.336	0.54 ± 0.01	−1.00 ± 0.14	...	*						
						0823 + 033	47939.164	1.14 ± 0.01	−1.30 ± 0.05	...	*
1309 − 217	48301.297	0.38 ± 0.01	−1.20 ± 0.12	...	*		48299.180	0.31 ± 0.01	−1.76 ± 0.15	...	
1400 + 162	47939.367	0.30 ± 0.01	−1.38 ± 0.05	...	*	0823 − 223	47167.289	1.97 ± 0.13	−1.08 ± 0.13	...	
							47168.309	1.93 ± 0.10	−0.94 ± 0.09	...	
1402 + 043	47569.352	0.72 ± 0.04	−0.72 ± 0.19	...			47526.293	1.62 ± 0.09	−0.96 ± 0.21	...	
	47939.320	0.46 ± 0.01	−1.06 ± 0.05	...			47569.160	1.25 ± 0.06	−0.99 ± 0.09	...	
	48299.340	0.65 ± 0.01	−1.08 ± 0.08	...	*		47942.301	...	−0.90 ± 0.05	...	
							48301.117	0.68 ± 0.03	−1.00 ± 0.08	...	*
1407 + 023	47941.488	...	−1.18 ± 0.12	...	*						
						0829 + 047	46803.313	1.27 ± 0.06	−1.43 ± 0.25	0.17	
							46805.316	1.09 ± 0.07	−1.34 ± 0.35	0.25	

TABLE 3—*Continued*

Name	MJD	F_ν(mJy)	α	P_g		Name	MJD	F_ν(mJy)	α	P_g	
1514 − 242	46682.984	3.34 ± 0.10	−1.13 ± 0.20	0.35		2005 − 489	47378.082	11.35 ± 0.17	−0.61 ± 0.05	...	
	47033.023	2.28 ± 0.20	−0.66 ± 0.30	0.45			47379.098	11.59 ± 0.14	−0.59 ± 0.05	...	
	47377.086	4.69 ± 0.14	−1.01 ± 0.20	0.30			47747.109	8.20 ± 0.04	−0.80 ± 0.05	...	
	47379.027	5.02 ± 0.14	−1.22 ± 0.15	0.20			47748.105	8.27 ± 0.05	−0.87 ± 0.05	...	
	47570.352	3.80 ± 0.08	−1.05 ± 0.15	0.30			47749.098	8.39 ± 0.05	−0.83 ± 0.05	...	
	47746.027	3.04 ± 0.04	−1.02 ± 0.15	0.40			48152.070	14.19 ± 0.11	−0.76 ± 0.05	...	*
	47750.039	2.97 ± 0.06	−1.15 ± 0.15	0.25	*		48155.066	13.47 ± 0.18	−0.64 ± 0.06	...	
1519 − 273	47747.984	0.08 ± 0.03	−0.93 ± 0.82	...	*	2012 − 017	47747.156	0.28 ± 0.01	−1.63 ± 0.12	...	*
1538 + 149	47377.035	0.39 ± 0.05	−1.85 ± 0.47	...		2155 − 304	46013.023	28.31 ± 0.52	−0.46 ± 0.05	...	
	47379.000	0.62 ± 0.06	−1.73 ± 0.33	...			46014.035	27.04 ± 0.62	−0.46 ± 0.05	...	
	47746.988	0.33 ± 0.01	−1.71 ± 0.08	...			46015.035	23.71 ± 0.52	−0.46 ± 0.05	...	
	47749.992	0.38 ± 0.02	−1.62 ± 0.16	...	*		46016.023	25.41 ± 0.59	−0.56 ± 0.05	...	
	48302.383	0.23 ± 0.04	−1.90 ± 0.80	...			46017.051	24.49 ± 0.57	−0.60 ± 0.05	...	
1553 + 113	46684.023	2.70 ± 0.12	−0.88 ± 0.12	...			46682.094	20.51 ± 0.40	−0.77 ± 0.05	...	
	47036.023	5.75 ± 0.10	−1.00 ± 0.07	...			46683.129	19.86 ± 0.32	−0.67 ± 0.05	...	
	47037.031	5.83 ± 0.16	−0.99 ± 0.08	...			46684.137	18.16 ± 0.35	−0.70 ± 0.05	...	
	47376.004	7.86 ± 0.14	−0.84 ± 0.06	...			47033.184	24.55 ± 0.45	−0.57 ± 0.05	...	
	47376.969	9.08 ± 0.13	−0.78 ± 0.05	...			47034.133	22.49 ± 0.33	−0.68 ± 0.05	...	
	47377.977	8.30 ± 0.12	−0.83 ± 0.05	...			47035.109	25.23 ± 0.38	−0.75 ± 0.05	...	
	47378.004	7.93 ± 0.13	−0.90 ± 0.06	...			47036.121	22.49 ± 0.33	−0.68 ± 0.05	...	
	47745.008	6.89 ± 0.05	−1.02 ± 0.05	...			47037.180	25.94 ± 0.39	−0.64 ± 0.05	...	
	47748.023	8.15 ± 0.05	−0.89 ± 0.05	...			47376.227	8.15 ± 0.11	−0.70 ± 0.05	...	
	47748.988	8.30 ± 0.05	−1.00 ± 0.05	...			47377.234	10.35 ± 0.19	−0.69 ± 0.05	...	
	48152.008	6.13 ± 0.09	−0.89 ± 0.05	...	*		47378.141	10.54 ± 0.14	−0.57 ± 0.05	...	
	48302.359	9.80 ± 0.10	−0.84 ± 0.05	...			47379.199	11.12 ± 0.15	−0.58 ± 0.05	...	
1722 + 119	47745.027	2.39 ± 0.02	−1.21 ± 0.05	...			47745.223	10.87 ± 0.05	−0.64 ± 0.05	...	
	47746.055	1.96 ± 0.03	−1.20 ± 0.05	...			47746.148	12.77 ± 0.16	−0.59 ± 0.05	...	
	47747.023	2.58 ± 0.02	−0.94 ± 0.05	...			47747.203	13.21 ± 0.18	−0.56 ± 0.05	...	
	47749.043	2.43 ± 0.02	−1.00 ± 0.05	...			47748.145	12.71 ± 0.17	−0.63 ± 0.05	...	
	48152.027	3.44 ± 0.03	−0.94 ± 0.05	...	*		47749.156	12.42 ± 0.15	−0.59 ± 0.05	...	
							48152.145	25.81 ± 0.35	−0.57 ± 0.05	...	*
1749 + 097	46683.059	0.99 ± 0.08	−0.75 ± 0.30	0.10		2201 + 044	46682.203	2.35 ± 0.09	−1.72 ± 0.60	0.90	
	47376.070	0.53 ± 0.05	−1.29 ± 0.20	0.24			47033.203	2.39 ± 0.23	−0.77 ± 0.40	0.80	
	47378.031	0.46 ± 0.04	−1.20 ± 0.20	0.32			47036.152	1.98 ± 0.16	−1.74 ± 0.60	0.90	
	47379.063	0.44 ± 0.06	−0.73 ± 0.20	0.34			47376.270	2.44 ± 0.13	−2.52 ± 0.50	0.80	
	47747.070	0.85 ± 0.01	−1.07 ± 0.15	0.14			47379.238	2.62 ± 0.14	−2.12 ± 0.50	0.90	
	47748.066	0.98 ± 0.01	−1.28 ± 0.12	0.10			47745.246	2.09 ± 0.03	−0.80 ± 0.30	0.85	
	47750.074	0.72 ± 0.02	−1.20 ± 0.12	0.12	*		47748.176	1.75 ± 0.03	−0.58 ± 0.60	0.85	*
						2208 − 137	47746.180	0.57 ± 0.02	+0.41 ± 0.12	...	
2005 − 489	46682.043	9.48 ± 0.22	−1.07 ± 0.05	...			47749.191	0.46 ± 0.02	+0.28 ± 0.12	...	*
	46683.102	8.93 ± 0.22	−0.97 ± 0.05	...							
	47033.109	10.19 ± 0.21	−0.69 ± 0.06	...		2223 − 052	47035.168	0.38 ± 0.15	−1.77 ± 0.80	...	
	47035.074	14.16 ± 0.19	−0.91 ± 0.05	...			47379.277	2.24 ± 0.06	−1.39 ± 0.09	...	
	47036.063	13.55 ± 0.17	−1.07 ± 0.05	...			47746.230	0.39 ± 0.02	−1.52 ± 0.09	...	
	47037.074	15.56 ± 0.21	−0.73 ± 0.05	...			47750.230	0.20 ± 0.01	−1.25 ± 0.11	...	*
	47376.133	10.54 ± 0.15	−0.76 ± 0.05	...							
	47377.141	11.64 ± 0.14	−0.73 ± 0.05	...							

TABLE 3—*Continued*

Name	MJD	F_ν(mJy)	α	P_g	
2230 + 115	47378.203	0.45 ± 0.04	−0.29 ± 0.43	...	*
2240 − 260	47377.289	0.40 ± 0.03	−1.71 ± 0.40	...	
	47747.250	0.20 ± 0.01	−1.63 ± 0.09	...	
	48152.188	0.18 ± 0.01	−1.53 ± 0.17	...	*
2254 + 075	47034.176	0.42 ± 0.18	−1.55 ± 0.30	0.20	
	47378.246	0.53 ± 0.05	−1.00 ± 0.30	0.50	
	47746.277	0.55 ± 0.01	−1.01 ± 0.20	0.45	
	47749.230	0.51 ± 0.02	−1.46 ± 0.20	0.35	*
2356 − 309	47747.301	0.46 ± 0.01	−1.80 ± 0.20	0.50	
	47748.230	0.45 ± 0.01	−1.90 ± 0.20	0.44	*

NOTE.—An asterisk (*) indicates that the observations are plottedin Figs. 1 and 2.

[3] Flux at 5500 Å, dots indicates poor photometry.

tributes 65% at 5500 Å. The absolute magnitude of the underlying galaxy, $M_V = -21.7 \pm 0.2$, confirms the previously reported values (Ulrich 1989) and is fully compatible with the value found in the optical to near-IR range (Falomo et al. 1993a).

0735+178.—This source is a typical BL Lac object, rapidly variable in the optical domain (Hufnagel & Bregman 1992). The continuum is featureless with the exception of a strong absorption at 3980 Å, which has already been detected and identified with Mg II (2798 Å) at $z = 0.424$ by Carswell et al. (1974). The spectral index remained nearly constant while the flux varied by ≃0.8 magnitudes.

0736+017.—This source, classified as blazar by Angel & Stockman (1980) shows strong permitted and forbidden emission lines in the optical domain, with FWHM ≃ 3000 km s^{-1} at $z = 0.191$. The continuum is flat and compatible with a power-law spectrum.

0754+101.—We obtained five spectra of this radio selected source, classified as blazar by Angel & Stockman (1980). The optical energy distribution is featureless. Despite large flux variations (up to 100%) the spectral index remained constant ($\Delta\alpha \lesssim 0.15$).

0808+019.—We obtained five spectra of this radio-selected BL Lac object (Angel & Stockman 1980) with unknown redshift. No spectral features were detected and the spectrum follows a power law very well. The flux show large variations ($\phi \simeq 2$), while the spectral index shows only little variability ($\Delta\alpha \lesssim 0.45$).

0818−128.—This radio-selected object has unknown redshift and we did not detect any structure in our five spectra. The continuum is well described by a power law with nearly constant spectral index, while the flux density shows large variations ($\phi \simeq 2$).

0823+033.—We observed this source, discovered in the polarimetric study of radio sources of Impey & Tapia (1988), at two very different flux levels ($\phi \simeq 3$). The spectra appear featureless and follow a power-law model very well. The spectral index decreases from −1.76 to −1.30 while the flux varied from 0.31 to 1.14 mJy in one year.

0823−223.—This high-redshift source, classified as blazar on the basis of its polarization properties (Impey & Tapia 1988), shows a typical power-law spectrum with no emission lines. We detected only Mg II (2798 Å) in absorption at $z = 0.910$. The spectral index is very stable ($\Delta\alpha \lesssim 0.2$) while the source exhibited a maximum flux variation of a factor 2.5.

0829+047.—This radio-selected BL Lac object shows very large flux variations (Liller & Liller 1975). The source is one of the most active in our sample, varying from 0.62 to 3.09 mJy ($\phi \simeq 4$). The optical spectra exhibit the signature of stellar emission at $z = 0.18$ (Falomo 1991a) with a mean contribution of 20%. The corresponding host galaxy absolute magnitude is $M_V = -22.7$, consistent with values found in the optical to near-IR range (Falomo et al. 1993a), but different from the value $M_V = -24.8$ determined by Abraham, Hardy, & Crawford (1991), on the basis of direct optical imaging. We observe large flux variability and the spectral index of the nonthermal component shows variations up to $\Delta\alpha \lesssim 0.6$ not correlated with the flux level.

0836+182.—The object, discovered by Wills & Wills (1979), exhibits a featureless spectrum well described by a power-law model.

0851+203.—OJ 287 is a typical BL Lac object that shows large optical bursts (Hufnagel & Bregman 1992). At low emission level permitted and forbidden emission lines are detected at $z = 0.306$ (Sitko & Junkkarien 1985). We observed OJ 287 four times and found flux variations of more than 200%. All spectra are well described by simple power law with a steep ($\alpha \simeq -1.4$) spectral index.

0906+016.—The spectrum of this radio-selected object shows a strong broad emission line at $\lambda \simeq 5650$ Å identified with Mg II 2798 Å at $z = 1.018$. The continuum emission is compatible with a power-law model.

1020−104.—The spectrum of this radio-selected OVV shows very strong emission lines. The continuum is flat ($\langle\alpha\rangle \simeq -0.28$) and described by a simple power-law model.

1055+018.—Two spectra were secured of this radio-selected blazar (Impey & Tapia 1988) at nearly the same flux level. The power-law spectra show only one clear structure, the Mg II 2798 Å emission line at $z = 0.888$ (Impey & Tapia 1988).

1057+101.—The spectrum of this blazar (Angel & Stockman 1980) shows two strong emission lines (Mg II 2798 Å and C III] 1909 Å) at $z = 1.317$ (Falomo 1991b), and a slightly curved continuum.

1101−232.—We obtained six spectra of this X-ray selected source (Remillard et al. 1989). Absorption features of Mg I ($\lambda = 5175$ Å) and Ca II ($\lambda = 3950$) are clearly detected at $z = 0.186$ which confirms the redshift proposed by Remillard et al. (1989). The optical continuum is well fitted by a power-law model plus a 30% contribution from the host galaxy. The corresponding absolute magnitude of the host galaxy is $M_V = -22.4 \pm 0.2$ consistent with the value $M_V = -22.2$ found in the optical to near-IR range (Falomo et al. 1993a).

1144−379.—Discovered in the polarimetric study of radio sources (Impey & Tapia 1988), 1144−379 is a high-redshift $z = 1.048$ (Stickel, Fried, & Kuhr 1989) radio-selected BL Lac object (Nicolas et al. 1979). We failed to detect any structure in the spectrum that are well described by a power law model.

1244−255.—Spectra of this radio-selected source (Impey & Tapia 1988) show a very strong emission line identified with Mg II (2798 Å) at $z = 0.638$. The optical energy distribution is described by a power law model.

TABLE 4

SUMMARY OF RESULTS

Name (1)	N_o (2)	N_c (3)	$\langle F_\nu \rangle$ (4)	ϕ (5)	$\langle \alpha \rangle$ (6)	α_{min} (7)	α_{max} (8)	R_s (9)	P_g (10)	$M_V\,gal$[4] (11)
0048 − 097	14	7	1.53	2.00	−0.92	−1.51	−0.72	−0.68	...	...
0109 + 225	3	3	0.94	2.21	−1.02	−1.06	−0.72	...	...	...
0118 − 273	10	5	1.35	1.63	−1.21	−1.39	−0.84	−0.20	...	...
0138 − 097	6	5	0.72	1.31	−1.02	−1.13	−0.85	−0.82	...	...
0215 + 015	2	1	3.93	0.13	−0.72	−0.77	−0.63	...	...	...
0301 − 244	6	5	1.20	1.12	−1.10	−1.23	−0.88	−0.40	...	...
0323 + 022	3	2	0.76	0.21	−0.25	−0.26	−0.22	...	0.19 - 0.33	−22.1
0338 − 215	6	5	0.80	0.45	−1.35	−1.51	−1.30	+0.80	...	...
0414 + 009	6	5	0.64	0.26	−0.37	−0.61	−0.15	+0.08	0.05 - 0.15	−22.2
0422 + 005	12	9	1.67	2.88	−1.37	−1.59	−1.10	−0.18	...	...
0521 − 365	16	10	2.63	1.16	−1.24	−1.62	−0.87	+0.24	0.45 - 0.68	−21.6
0537 − 441	14	9	1.33	3.10	−1.08	−1.65	−1.06	−0.25	...	...
0548 − 323	6	6	1.30	0.20	−0.52	−1.05	−0.13	...	0.60 - 0.70	−21.7
0735 + 178	3	3	1.48	1.08	−1.24	−1.40	−1.23	...	...	...
0736 + 017	1	1	0.73	...	−0.08	...	...	...	...	...
0754 + 101	5	5	2.50	1.30	−1.11	−1.24	−1.10	−0.50	...	...
0808 + 019	5	3	0.77	1.86	−0.94	−1.08	−0.63	...	...	...
0818 − 128	5	5	0.59	2.03	−0.88	−1.21	−0.75	...	...	...
0823 + 033	2	2	0.73	2.68	−1.35	−1.76	−1.30	...	...	...
0823 − 223	6	5	1.49	1.89	−0.93	−1.08	−0.90	+0.01	...	...
0829 + 047	7	4	1.52	3.98	−1.08	−1.43	−0.83	+0.40	0.13 - 0.30	−22.7
0836 + 182	1	1	0.19	...	−1.58	...	...	...	...	...
0851 + 203	4	3	2.06	2.42	−1.43	−1.61	−1.18	...	...	...
0906 + 016	1	1	0.28	...	−0.55	...	...	...	...	...
1020 − 104	3	3	0.74	0.05	−0.28	−0.42	−0.14	...	...	...
1055 + 018	2	2	0.38	0.08	−1.38	−1.39	−1.32	...	...	...
1057 + 101	2	1	0.35	...	−0.58	−0.58	−0.57	...	...	...
1101 − 232	6	3	0.54	0.37	−0.48	−0.69	−0.25	...	0.20 - 0.35	−22.4
1144 − 379	3	3	0.60	0.54	−1.05	−1.17	−1.00	...	...	...
1244 − 255	3	3	0.69	0.54	−0.99	−1.09	−0.64	...	...	...
1309 − 217	1	1	0.38	...	−1.20	...	...	...	...	...
1400 + 162	1	1	0.30	...	−1.38	...	...	...	...	...
1402 + 043	3	3	0.61	0.56	−1.06	−1.08	−0.72	...	...	...
1407 + 023	1	1	...	...	−1.18	...	...	...	...	...
1514 − 242	7	5	3.59	1.20	−1.08	−1.22	−0.66	+0.40	0.20 - 0.45	−21.6
1519 − 273	1	1	0.08	...	−0.93	...	...	...	...	...
1538 + 149	5	3	0.39	1.69	−1.70	−1.90	−1.62	−0.20	...	...
1553 + 113	12	6	7.23	2.63	−0.96	−1.02	−0.78	−0.48	...	...
1722 + 119	5	2	2.56	0.75	−1.05	−1.21	−0.94	...	...	...
1749 + 097	7	3	0.71	1.25	−1.15	−1.29	−0.73	−0.28	0.10 - 0.34	−23.4
2005 − 489	15	5	11.30	0.90	−0.82	−1.07	−0.59	−0.23	...	...
2012 − 017	1	1	0.28	...	−1.63	...	...	...	...	...
2155 − 304	23	6	18.96	2.47	−0.62	−0.77	−0.46	−0.36	...	...
2201 + 044	7	4	2.23	0.50	−1.29	−2.52	−0.58	+0.64	0.90 - 0.80	−20.7
2208 − 137	2	1	0.52	0.24	+0.34	+0.28	+0.41	...	...	...
2223 − 052	4	3	0.80	10.20	−1.41	−1.77	−1.25	...	...	...
2230 + 115	1	1	0.45	...	−0.29	...	...	...	...	...
2240 − 260	3	3	0.26	1.22	−1.61	−1.71	−1.53	...	...	...
2254 + 075	4	3	0.50	0.31	−1.25	−1.55	−1.00	...	0.20 - 0.50	−22.5
2356 − 309	2	1	0.46	0.02	−0.37	−0.62	−0.12	...	0.44 - 0.50	−22.2

[4] Values are corrected for Galactic extinction but not *K*-corrected.

1309−217.—We did not detect emission or absorption lines in the spectra of this radio-selected object (Impey & Tapia 1988). The continuum is well described by a simple power law.

1400+162.—Spectra of this radio-selected blazar (Angel & Stockman 1980) are structureless and well described by a power law.

1402+042.—The continuum of this X-ray selected BL Lac objects is structureless. We observed the source at two flux levels finding that the energy distribution is described by a power law with a relatively steep spectral index.

1407+022.—A power-law model ($\alpha \simeq -1$) describes the featureless emission of this radio selected BL Lac object of unknown redshift.

1514−242.—AP Librae is a classical radio-selected object (Strittmatter et al. 1972). We observed the source on seven occasions and found flux variability of up to 1 magnitude. The optical energy distribution clearly shows the presence of a ther-

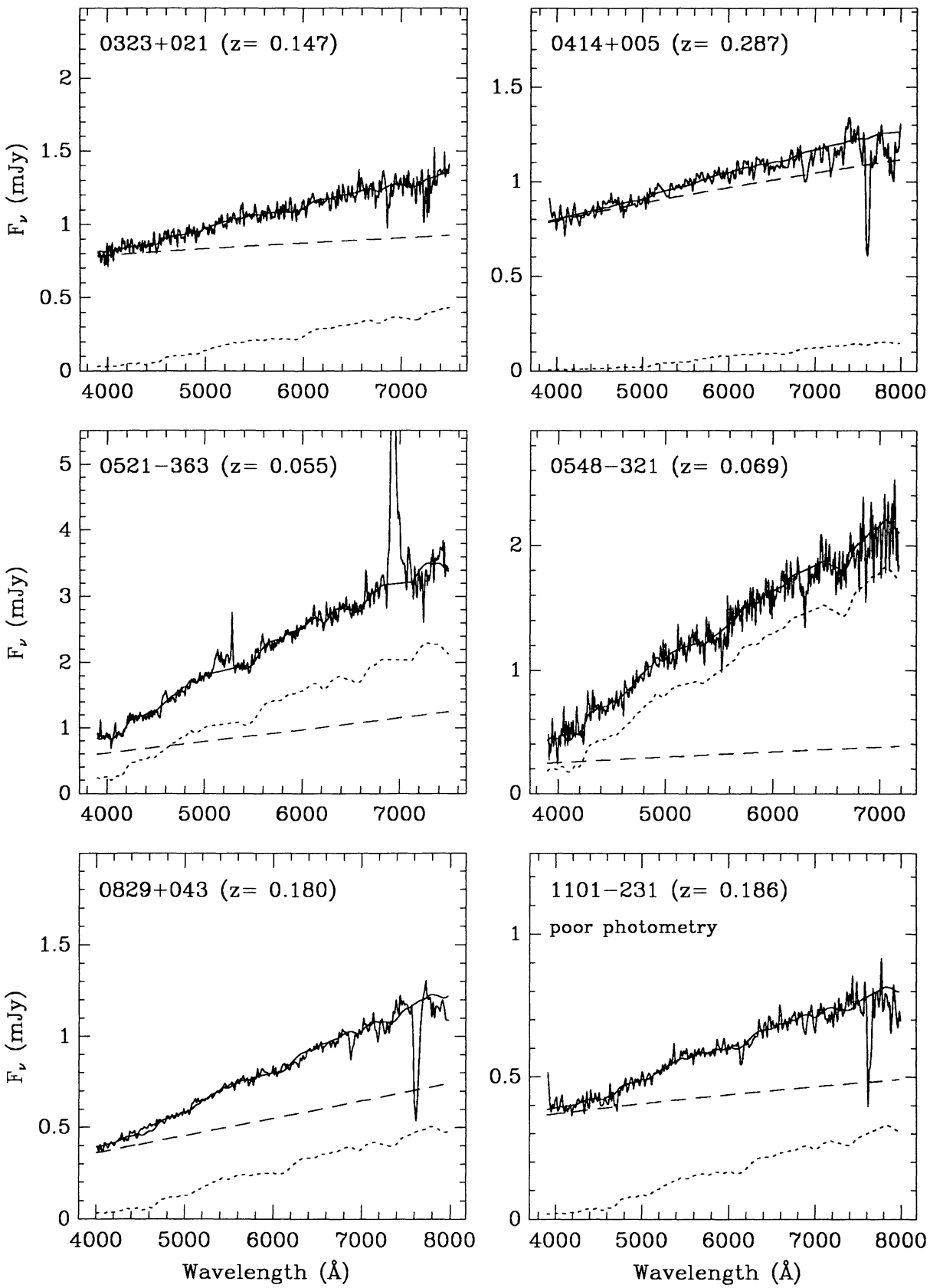

FIG. 2.—Decomposition of spectral flux distribution for objects with a significant host galaxy component. Spectra were corrected for interstellar extinction according to values of A_V reported in Table 2. The spectra are decomposed into starlight (*dotted line*) and nonthermal (*dashed line*) components. The resulting best fit (*solid line*) is also shown. Spectra plotted are marked with an asterisk (*) in Table 3.

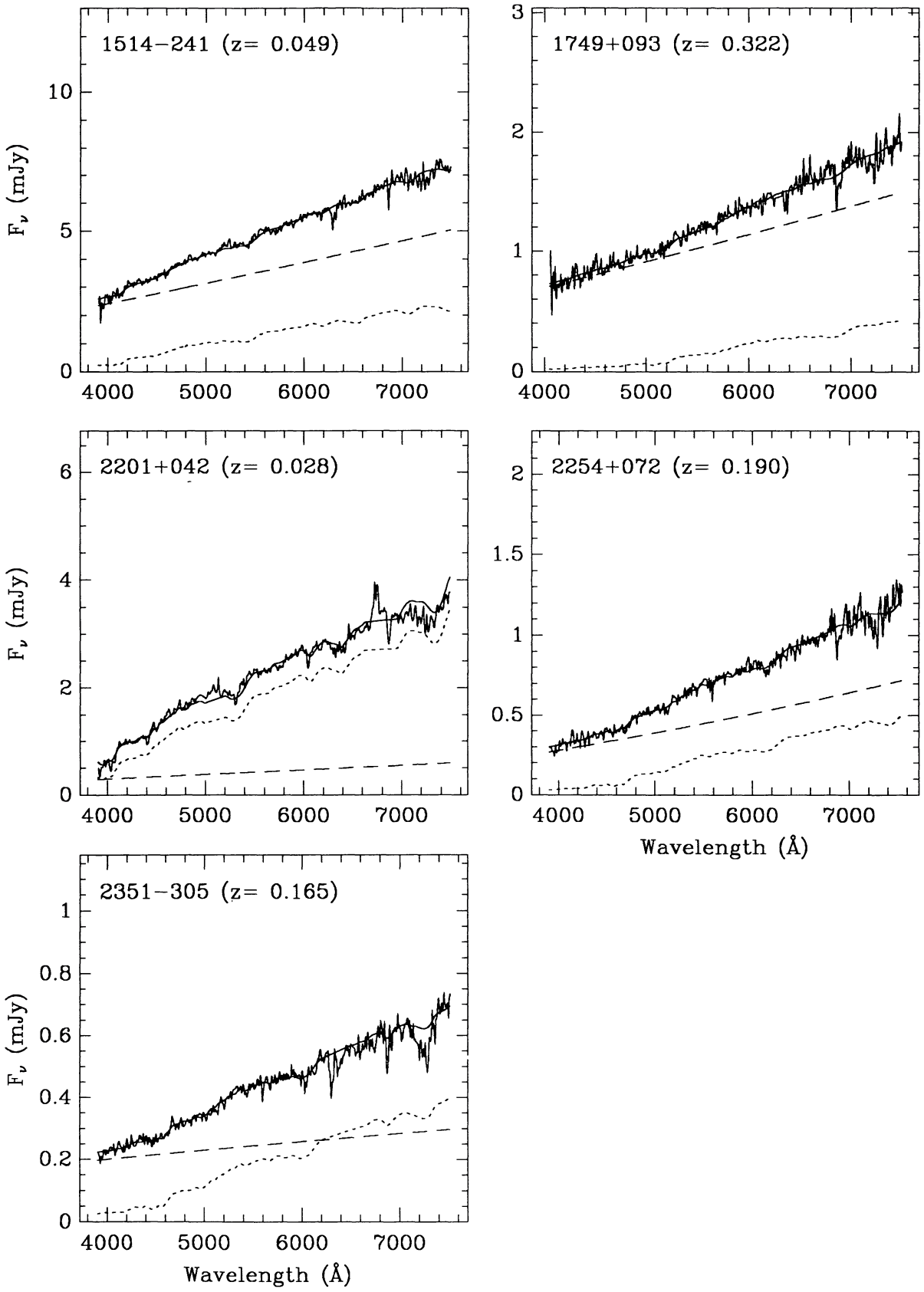

FIG. 2—*Continued*

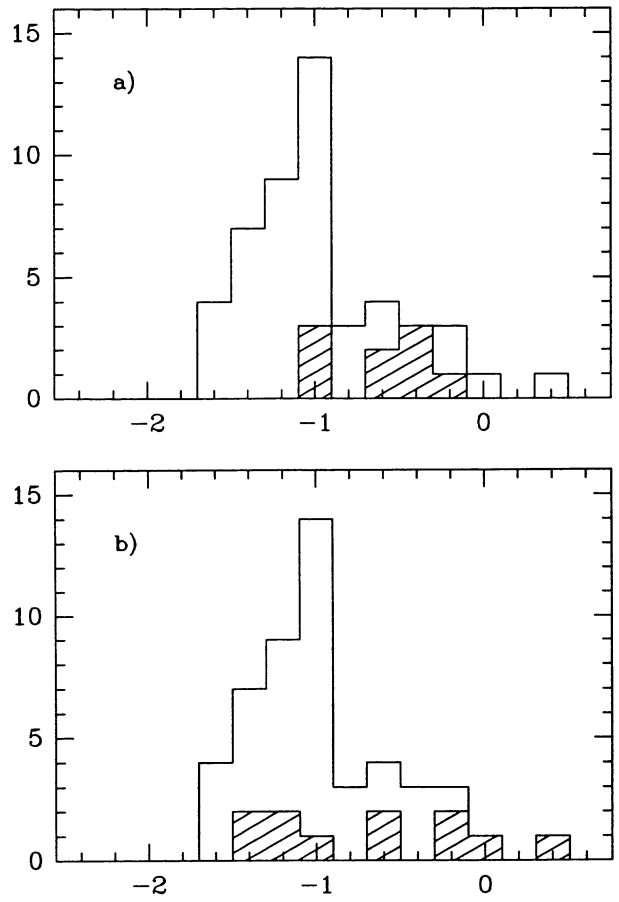

FIG. 3.—Distribution of optical spectral indices. (*a*) Radio-selected objects compared to X-ray selected objects (*shaded area*). (*b*) Weak-line objects compared to strong-line objects (*shaded area*).

mal component from a host galaxy, which contributes 33% of total flux. The spectral index remained practically constant; only in the observation of 1987 August, at the minimum detected flux level, did we observe a spectral index significantly flatter. The host galaxy absolute magnitude is $M_V = -21.6 \pm 0.2$. This value is in agreement with all the previously reported values (Ulrich 1989; Abraham et al. 1991; Falomo et al. 1993a; Stickel et al. 1993).

1519−273.—We obtained one spectrum of this faint ($m_V \sim 19$) radio-selected object with unknown redshift. We found that the energy distribution is structureless (in agreement with White et al. 1988) and well represented by a simple power-law model.

1538+149.—The flux density of this radio-selected blazar (Angel & Stockman 1980) shows large variations (more than 1 magnitude) while the spectral index remained essentially unchanged ($\Delta\alpha \lesssim 0.28$). The energy distribution is the steepest ($\alpha \lesssim -1.7$) observed in our sample.

1553+113.—We repeatedly observed this bright X-ray selected object obtaining 12 spectra, all described by a power law with $\alpha \simeq -1$. The continuum is featureless. The magnitude varied by $\Delta m = 1.4$ in 5 years. In the same period the spectral index remained nearly constant showing a maximum variation of 0.24.

1722+119.—The optical continuum of this X-ray selected object recently discovered by Brissenden et al. (1990), is well described by a power-law model with stable spectral index ($\Delta\alpha \lesssim 0.27$). We have observed this source 4 times in 4 consecutive nights finding a variation of 0.3 magnitudes.

1749+096.—We observed this radio selected BL Lac in a large range of luminosity. The spectral index showed large variations ($\Delta\alpha \simeq 1.4$) correlated with flux density. This effect, however, is readily explained by the strong variation of the relative emission from the host galaxy and the nonthermal component. When the power-law emission is maximum the spectrum is flat and, vice versa, at minimum the red part of the spectrum is enhanced because the stellar emission is stronger at these wavelengths. After accounting for the thermal emission, spectral index variability is largely reduced ($\Delta\alpha \lesssim 0.55$) and the correlation disappears. The thermal component from the host galaxy contributes on average 20% of the total. The corresponding absolute magnitude of the galaxy is $M_V = -23.4$. This is the only case of a marked discrepancy ($\Delta m_V \sim -0.8$) with the values of M_V estimated by Falomo et al. (1993a).

2005−489.—Even though this bright radio source is well resolved in direct images, which show a large elliptical nebulosity (Wall et al. 1986), our 15 spectra of the source are all described by a simple power law, indicating that the central source is largely dominant. The flux density exhibited changes up to 100% while the spectral index shows variations smaller than 0.5.

2012−017.—We obtained only one spectrum of this radio-selected source, which is featureless and well described by a power law with a steep ($\alpha \simeq -1.6$) spectral index.

2155−304.—This bright ($m_V \simeq 13$) X-ray selected BL Lac object, was discovered as the optical counterpart of the X-ray source H2155−30 by Griffiths et al. (1979). We have repeatedly observed this object obtaining as many as 23 spectra over six campaigns. The source showed flux variability on long timescales ($\Delta m = 1.3$) but remained quite stable on short timescales. At all flux levels spectra are well described by a power-law model with nearly constant ($\Delta\alpha \lesssim 0.3$) spectral index. Note that the structure observed at ~5700 Å is due to a small residual from the grating efficiency calibration.

2201+044.—This is a nearby $z = 0.028$ source classified as a BL Lac (Angel & Stockman 1980). We find that in the optical range emission from the host galaxy is very strong representing on average 85% of the total flux. This is responsible for the very large error in the spectral index determination; thus the minimum value ($\alpha_{min} = -2.5$) is highly uncertain. Decomposition gives a host galaxy magnitude of $M_V = -20.7 \pm 0.2$ consistent

TABLE 5

MEAN SPECTRAL INDICES OF SUBCLASSES

Subclass	$\langle\alpha\rangle$[a]	$N_{objects}$
All	−0.98 ± 0.43	(50)
Radio-selected	−1.05 ± 0.42	(40)
X-ray selected	−0.65 ± 0.30	(10)
Weak emission lines	−1.05 ± 0.35	(37)
Strong emission lines	−0.75 ± 0.57	(13)

[a] The quoted errors are the sample variances (rms) of the distributions.

with −20.8 found in the optical to near-IR range (Falomo et al. 1993a).

2208−137.—This radio-selected blazar (Moore & Stockman 1981) is the only object in our sample that shows a positive spectral index. The spectra exhibit strong broad Balmer emission lines while the [O III] emission lines are narrow. The continuum is consistent with a power law model.

2223−052.—The weak-lined, high-redshift $z = 1.404$ (Burbidge, Crowne, & Smith 1977) and high-luminosity blazar 3C 446 is a well-known object, intermediate between a typical BL Lac and the strong-lined objects like 3C 345 (Bregman et al. 1988). This source is one of the most luminous QSOs known and yet is one of the most rapidly variable (Hufnagel & Bregman 1992). We obtained four spectra, all described by a power law model, at very different flux levels, observing a variation of more than 2.5 magnitudes (the largest observed in our sample).

2230+115.—The spectrum of this radio-selected object is curved and only marginally consistent with a power law. We detected a strong emission line at $\lambda \simeq 5715$ Å which if due to Mg II ($\lambda = 2798$) gives $z = 1.037$.

2240−260.—No emission lines are found at $z = 0.774$, as proposed by Stickel et al. (1993) on the basis of very weak emission lines. A power-law model with constant spectral index describes well the featureless spectrum while the flux density varied by more than a factor of 2.

2254+074.—This object is resolved in direct images (Craine, Tapia, & Talenghi 1975; Stickel et al. 1993) showing the surrounding host galaxy. We found that spectra clearly exhibit the presence of the thermal component with a mean contribution of 37%. We deduced a host galaxy magnitude of $M_V = -22.5 \pm 0.2$, compatible with the value $M_V = -22.5 \pm 0.2$ found by Falomo et al. (1993a), but substantially smaller than $M_V \simeq -23.3$ found by Stickel et al. (1993) and by Romanishin (1987). The spectral index shows variations up to 0.5.

2356−309.—This X-ray selected source detected by the *Uhuru* satellite was identified with a $m_V \sim 17$ BL Lac object by Schwartz et al. (1989). The observed spectra show the clear signature of the underlying galaxy. The energy distribution is well described by a power law plus 50% thermal emission. The resulting absolute magnitude of the host galaxy is -22.2 ± 0.2 in agreement with the one estimated from direct imaging by Falomo (1991a).

We thank J. E. Pesce for useful suggestions on the text and M. Calvani for his availability and assistance in using graphic facilities. This research has made use of the NASA/IPAC Extragalactic Database (NED) which is operating by the Jet Propulsion Laboratory, Caltech, under contract with the National Aeronautics and Space Administration, and of the graphics package Super Mongo by R. Lupton and P. Monger.

REFERENCES

Abraham, R. G., Hardy, I. M. M., & Crawford, C. S. 1991, MNRAS, 252, 482
Angel, J. R. P., & Stockman, H. S. 1980, ARA&A, 18, 321
Ballard, K. R., Mead, A. R. G., & Brand, P. W. J. L. 1990, MNRAS, 243, 640
Bersanelli, M., Bouchet, P., Falomo, R., & Tanzi, E. G. 1992, AJ, 104, 28
Boissé, P., & Bergeron, J. 1988, A&A, 192, 1
Boisson, C., Cayatte, V., & Sol, H. 1989, A&A, 211, 275
Bregman, J. N. 1990, ARA&A, 2, 125
Bregman, J. N., et al. 1988, ApJ, 331, 746
Brissenden, R. J. V., et al. 1990, ApJ, 350, 578
Brown, L. M. J., Robson, E. J., Gear, W. K., & Smith, M. G. 1989, ApJ, 340, 150
Burbidge, G. R., Crowne, A. H., & Smith, H. E. 1977, ApJS, 33, 113
Cardelli, J. A., Clayton, G. C., & Mathis, J. S. 1989, ApJ, 345, 245
Carswell, R. F., et al. 1974, ApJ, 190, L101
Choen, M. H., et al. 1977, Nature, 268, 405
Craine, E. R., Tapia, S., & Talenghi, M. 1975, Nature, 258, 56
Cruz Gonzales, J., & Huchra, J. P. 1984, AJ, 89, 441
Danziger, I. J., Fosbury, R. A. E., Goss, W. M., & Ekers, R. D. 1979, MNRAS, 188, 415
Elvis, M., Lockman, F. J., & Wilkes, B. J. 1989, AJ, 97, 777
Edelson, R., et al. 1992, ApJS, 83, 1
Falomo, R. 1990, Nature, 345, 692
———. 1991a, AJ, 101, 821
———. 1991b, AJ, 102, 1991
Falomo, R., Bersanelli, M., Bouchet, P., & Tanzi, E. G. 1993a, AJ, 106, 11
Falomo, R., & Treves, A. 1990, PASP, 102, 1120
Falomo, R., Treves, A., Chiappetti, L., Maraschi, L., Pian, E., & Tanzi, E. G. 1993b, ApJ, 402, 532
Feigelson, E. D., et al. 1986, ApJ, 302, 337
Ghisellini, G., Maraschi, L., Tanzi, E. G., & Treves, A. 1986, ApJ, 310, 317
Griffiths, R. E., Tapia, S., Briel, U., & Chaisson, L. 1979, ApJ, 234, 810
Hufnagel, B. R., & Bregman, J. N. 1992, ApJ, 386, 473
Impey, C. D., & Neugebauer, G. 1988, AJ, 95, 307
Impey, C. D., & Tapia, S. 1988, ApJ, 333, 666
Jones, T. W., O'Dell, S. L., & Stein, W. A. 1974, ApJ, 188, 345
Ledden, J. E., & O'Dell, S. L. 1985, ApJ, 298, 630
Liller, M. H., & Liller, W. 1975, ApJ, 199, L133
Lorenzetti, D., et al. 1990, A&A, 235, 35
Mead, A. R. G., et al. 1990, A&AS, 83, 183
Miller, J. S., French, H. B., & Hawley, S. A. 1987, in Pittsburgh Conf. BL Lac Objects, ed. A. M. Wolfe (Pittsburgh: Univ. Pittsburgh), 176
Moore, R. L., & Stockman, H. S. 1981, ApJ, 243, 60
Nicolas, G. D., Glass, I. S., Feast, M. W., & Andrews, P. J. 1979, MNRAS, 189, 29P
O'Dell, S. L., et al. 1978, ApJ, 224, 22
Remillard, R. A., Tuohy, I. R., Brissenden, R. J. V., Buckely, D. A. H., Schwartz, D. A., Feigelson, E. D., & Tapia, S. 1989, ApJ, 345, 140
Rieke, G. H., & Lebofsky, M. 1985, ApJ, 288, 618
Romanishin, W. 1987, ApJ, 320, 586
Schwartz, D. A., et al. 1989, BAAS, 21, 777
Shull, J. M., & Van Steenberg, M. E. 1985, ApJ, 294, 599
Sitko, M. L., & Junkkarien, V. T. 1985, PASP, 97, 1158
Sitko, M. L., & Sitko, A. K. 1991, PASP, 103, 160
Stark, A. A., Gammie, C. F., Wilson, R. W., Bally, J., Linke, R. A., Heiles, C., & Hurwitz, M. 1992, ApJS, 79, 77
Stickel, M., Fried, J. W., & Kuhr, H. 1989, A&AS, 80, 103
———. 1993, A&AS, 98, 393
Stone, R. P. S. 1977, ApJ, 218, 767
Strittmatter, P. A., et al. 1972, ApJ, 175, L7
Tanzi, E. G., et al. 1989, in Lecture Notes in Physics, Vol. 334, BL Lac Objects, ed. L. Maraschi, T. Maccaro, & M. H. Ulrich (Berlin: Springer), 73
Ulmer, M. P., et al. 1983, ApJ, 270, L1
Ulrich, M. H. 1989, in Lecture Notes in Physics, Vol. 334, BL Lac Objects, ed. L. Maraschi, T. Maccaro, & M. H. Ulrich (Berlin: Springer), 45
Wall, J. V., et al. 1986, MNRAS, 219, 23P
Weistrop, D., Shaffer, D. B., Mushotzky, R. F., Reitsema, H. J., & Smith, B. A. 1981, ApJ, 249, 3
White, G. L., et al. 1988, ApJ, 327, 561
Wilkes, B. J., Wright, A. E., Jauncey, D. L., & Peterson, B. A. 1983, Proc. Astron. Soc. Australia, 5, 2
Wills, B. J., & Wills, D. 1979, ApJS, 41, 689
Wills, D., & Wills, B. J. 1976, ApJS, 31, 143
Yee, H. K. C., & Oke, J. B. 1978, ApJ, 226, 753